



Rain, wind or fire: which led the PAH fallout in Northern Madagascar across the Holocene?

5 Emeline Bellet¹, Vincent Montade², Christine Piot¹, Guillemette Ménot³, Aimée Pellissier-Tanon^{1,4},
Ilham Bentaleb², Hermann Behling⁵, Charline Giguet -Covex¹, Laurent Brémond² and Fabien Arnaud¹

1. EDYTEM, Université Savoie Mont-Blanc, CNRS, Chambéry, France

2. ISEM, University of Montpellier, CNRS, IRD, EPHE, PSL Research University, Montpellier, France

10 3. ENS Lyon, UCBL, CNRS, UMR 5276 LGL-TPE, Lyon, France

4. Department of Earth System Sciences, University of Hamburg, Hamburg, Germany

5. Department of Palynology and Climate Dynamics, Georg-August-Universität Göttingen, Göttingen, Germany

Correspondence to: Emeline Bellet (emeline.bellet@univ-smb.fr)

15

Abstract.

The interactions between wildfire, human and climate variability are not well understood. To have better
predictions, past studies are useful for observing their behaviours on a long-time scale. To infer past fire activity,
studies used charcoal and molecular biomarkers derived from biomass burning, such as Polycyclic Aromatic
20 Hydrocarbons (PAHs). In the north of Madagascar, charcoals are of local origin and have shown increased
abundance since 1000 cal a BP. In contrast, PAH are present throughout the Holocene. Therefore, PAHs likely
provide a more regional information. Due to the seasonal wind regime, they are thought to originate from East
Africa. However, the PAH signal pattern differs from the fire activity record of East Africa. Instead, it shows a
similar pattern to precipitation variability in northern Madagascar. Higher PAH concentrations are observed during
25 wetter period, whereas lower concentrations occur during drier periods. This suggest that PAH preservation is
enhanced, which may facilitate leaching processes prior to their deposition in sediments. These results challenge
the direct interpretation of PAH as straightforward indicators of fire events and dry periods.

30

1. Introduction

Worldwide, wildfire frequencies and burned areas tend to increase with temperature rise (IPCC, 2022). However,
the interactions between wildfire dynamics and human land uses, climate, and environmental perturbations,
particularly in the tropics, are not well understood (Brémond et al., 2024; Daniau and Brücher, 2016; Denis et al.,
35 2012). Therefore, past studies can provide a better understanding of wildfire behaviour and improve predictions
(Daniau and Brücher, 2016; Karp et al., 2020a).

Past wildfire reconstructions are generally based on charcoal counting and black carbon assessment in sediment
records (Daniau and Brücher, 2016; Karp et al., 2020a; Strobel et al., 2024). Charcoal abundance, shape, size, and
reflectance can give information on the severity and fuel sources of the palaeo-fire. However, those interpretations
40 can be biased due to the nature of the source fuels (Thevenon, 2003), and gaps remain regarding regional and
isolated fires, the areas burned, and the distinction between human and climatic factors underlying the fires. To
bring new information and complement charcoal records, more and more studies focus on fire-derived organic



45 molecules (Battistel et al., 2017; Karp et al., 2020a; Strobel et al., 2024; Yamamoto et al., 2022). Among them, Polycyclic Aromatic Hydrocarbons (PAHs) are a group of hydrophobic molecules, composed of 2 to 8 aromatic rings, which mostly derive from the incomplete combustion of organic matter (Lima et al., 2005). Their sources can be natural (e.g., volcanic activity, wildfires) but are also strongly linked to human activities. Their low solubility limits degradation, allowing good preservation in sediment cores (Karp et al., 2020a), whereas their high volatility leads them to spread over long-distances, depending on air-mass trajectories. As such, PAHs are increasingly used as biomarkers of human impact in historical records (Denis et al., 2012; Miller et al., 2017; 50 Vachula et al., 2022) and for palaeo-fire activity reconstructions (Argiriadis et al., 2024; Battistel et al., 2017; Karp et al., 2020a; Strobel et al., 2024; Yamamoto et al., 2022). Their abundances and relative composition indeed give information on fire fuel, fire intensity, and combustion temperature (Battistel et al., 2017; Denis et al., 2012; Strobel et al., 2024; Yamamoto et al., 2022). However, those interpretations are based on fire experiments or observations, realised by a limited set of fuel types and burned conditions (Karp et al., 2020a; Wilcke et al., 2002). 55 Therefore, gaps remain in how interpret PAHs in sediment cores. Those gaps are the result of the diversity of PAHs and their physico-chemical characteristics.

PAHs present different dispersion pathways within the environment after their emission from wildfires, mainly depending on their molecular weight: lower molecular weight (LMW) PAH travel in a gaseous form, whereas higher molecular weight (HMW) PAH travel as particles. Therefore, LMW PAH can travel over long distances 60 (Cabrerizo et al., 2014; Halsall et al., 2001) and are better suited to reconstruct regional fires than charcoals (Cabrerizo et al., 2014; Halsall et al., 2001; Vachula et al., 2022). The high volatility of PAHs tends to concentrate them within the atmosphere until the water condensation causes to their fallout, accompanying rainfalls. Indeed, current observations indicate that wet deposits are more substantial than dry depositions (Marçais, 2017). This observation was confirmed over the historic period by Denis et al. (2012), who led a comparative analysis of 65 sedimentary PAHs and historical data and also concluded that precipitation facilitated the scavenging of PAHs from the atmosphere to the Earth's surface and ultimately to lacustrine sediments. As the condensation pathway dominates the PAH fallout, their deposition flux in a given location partially depends on local climatic conditions and their changes through time. As a consequence, it is not clear whether the distant emission flux of PAHs or the local precipitation changes drive the PAH record in a given natural archive. In order to address this question, we 70 studied the sediment of Lake Maudit, located in the North of Madagascar. This region has both experienced known drastic precipitation changes throughout the Holocene and is susceptible to receiving a substantial flux of PAHs from the nearby African continent during monsoon months.

75 In northern Madagascar, charcoal counting has shown that wildfire frequency drastically rose between 1500 and 1000 cal a BP (Matsumoto and Burney, 1994; Montade et al., 2024; Reinhardt et al., 2022) in response to a generalised rise in grass combustion (Montade et al., 2024; Teixeira et al., 2021). Those changes occurred synchronously with the increase in human presence, and have also been proposed as reflecting a subsistence shift from hunter-gatherer to pastoralist activity (Douglass et al., 2019; Godfrey et al., 2019; Montade et al., 2024; 80 Teixeira et al., 2021). Nonetheless, a question persists regarding whether the fires and environmental changes observed 1,000 years ago were caused by human activity or by a severe drought (Montade et al., 2024) or through a combination of both factors. Before this date virtually no charcoals was found in the sediment record (Matsumoto and Burney, 1994; Montade et al., 2024; Reinhardt et al., 2022).

85 In parallel, Holocene changes in precipitation have been assessed through the $\delta^{18}\text{O}$ signal from a speleothem in Anjohibe Cave (Fig. 1). Those results suggest wetter conditions during the Early Holocene and drier conditions during the Mid and Late Holocene (Dawson et al., 2024; Wang et al., 2019). Comparable outcomes were observed in the investigation of pollen and sediment records from Lake Maudit (Teixeira et al., 2021). It hence seems that during the Early Holocene, the wetter conditions observed in continental Africa (Tierney et al., 2011) also reached



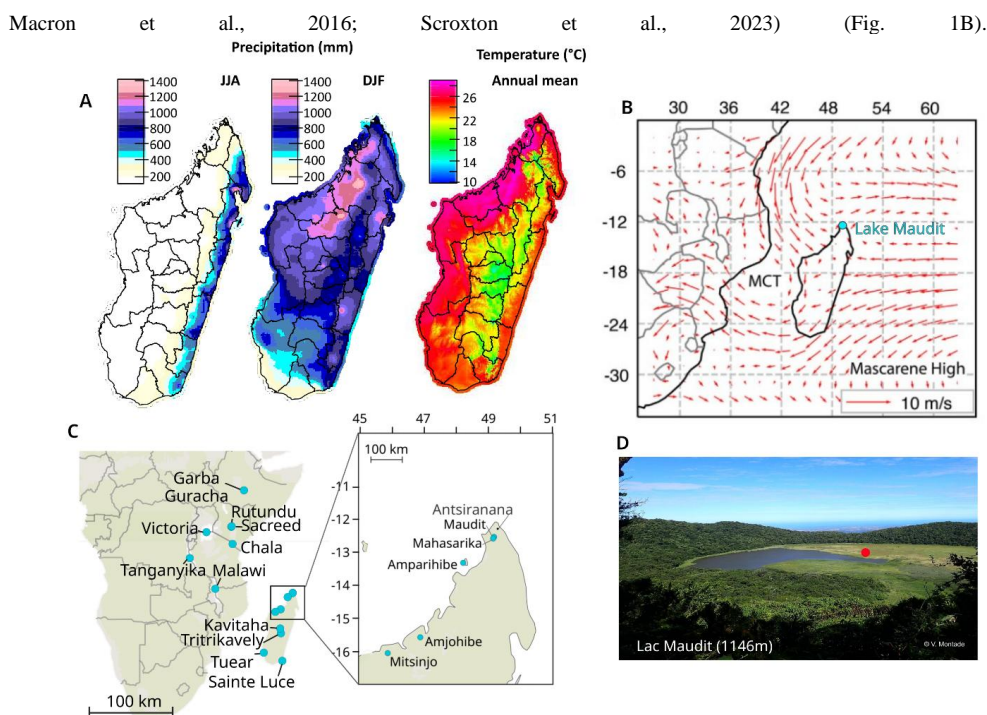
90 the North of Madagascar (Montade et al., 2024; Teixeira et al., 2021; Wang et al., 2019). Furthermore, there is
increasing evidence of two significant droughts occurring approximately 4000 and 1000 cal a BP (Douglass et al.,
2019; Li et al., 2020b; Montade et al., 2024; Vallet-Coulomb et al., 2006; Virah-Sawmy et al., 2010; Wang et al.,
2019). Based on this knowledge, we take advantage of known climatic and local wildfire frameworks of northern
Madagascar to investigate PAH deposition pathways over the whole Holocene. We hence aim at defining the local
95 vs. distant origin of PAHs and determining whether local or distant wildfire activity, or local precipitation patterns,
drive the PAH deposition fluxes.

2. Materials and methods

2.1. Region description

100

The island of Madagascar experiences a marked seasonality in its wind regime, which influence the precipitation
pattern, with a dry season from May to November and a wet season from December to April (Fig. 1A). During the
austral winter (June-August), the Mascarene subtropical high-pressure cell is intense and generates strong south-
easterly trade winds, bringing wet air to Madagascar (Fleitmann et al., 2007; Joly, 1941; Jury, 2016; Jury et al.,
105 1995; Macron et al., 2016). The mountain ridge (>1500 m), which crosses the island from the North to the South,
stops the trade winds, which are deviated to the North (Jury, 2016; Jury et al., 1995; Macron et al., 2016). This
leads to a marked rainfall gradient from the East to the West. As a result, the eastern part receives 3 to 4 times
more precipitation than the western part of the island (Jury, 2016; Macron et al., 2016) (Fig.1A). During the austral
summer (December – February), the Mascarene high-pressure system weakens, resulting in weaker trade winds.
110 This allows the Intertropical Convergence Zone (ITCZ) and its associated deep tropical convection to migrate
southward into the Mozambique Channel and the north of Madagascar (Jury, 2016; Macron et al., 2016; Scroxton
et al., 2023). In the north of Madagascar, the south-easterly trade winds curve and become north-westerlies
(Fig.1B) (Fleitmann et al., 2007; Scroxton et al., 2023). Toward the island, they transport the seasonal summer
precipitation, named the Malagasy Summer Monsoon (MSM). Consequently, a net gradient of precipitation is
115 observed, with the northern part of the island receiving more rainfall than the South (Jury, 2016; Jury et al., 1995;



120 *Figure 1 : Study area. A. Current mean meteorological conditions over the period 1950-2000. Data were extracted from the MadaClim database (<https://map.meteomadagascar.mg/maproom/Climatology/>). B. Wind in the region and over Lake Maudit (blue dot) based on ERA5 (fifth generation European reanalysis data (Hersbach et al., 2020)) at the 850 hectopascal (hPa) atmospheric pressure level with January mean wind direction and strength (red arrows) with Mozambique Channel Trough (MCT) and Mascarene High labeled. (from Dawson et al. 2024). C: Map of East Africa and Madagascar showing the location of Lake Maudit and the principal features discussed in this study. D. Photograph of Lake Maudit ©Vincent Montade. Red dot represents the location of the coring site. Note the current peat spread over the lake.*

130 2.2. Lake Maudit paleoenvironmental record

135 Lake Maudit (−12.582°N, 49.150°E, 1250 m asl) is a mountain lake, located in the Montagne d’Ambre massif at 1149 m asl (Fig. 1C). Here, the observed mean annual air temperature is 19°C, compared to 28°C close to the coast. The lake is of volcanic origin and, as such, is roughly circular, with a diameter of ca. 500 m (Fig. 1A). For this study, we use the 11 m sediment cores LM1A and LM1B, taken in 2017 using a Russian corer (Teixeira et al., 2021). A previous study showed that the sedimentary record covers the last 25,000 years (Teixeira et al., 2021). Over the Holocene, this pollen-based reconstruction evidenced the strong influence of the East African Humid Period (EAHP) on vegetation between 15,200 and 5,000 cal BP (Teixeira et al., 2021). Indeed, Teixeira et al. (2021) inferred a clear change in vegetation at 15,200 cal a BP, passing from mountain vegetation to an evergreen humid forest. The mountain vegetation was less widespread since 11,800 cal a BP. Although the evergreen humid forest remained stable until 900 cal a BP, vegetation succession appeared. The species assemblage suggested higher precipitation between 11,800 and 5500 cal a BP, coinciding with an increase in chemical weathering. From



5500 cal a BP, the diminution in chemical weathering, combined with a lake-level decrease and an increase in arboreal pioneer species, supports a reduction in precipitation, highlighting the end of the AHP (Teixeira et al., 2021). Finally, from ca. 1000 yr ago, an increase in Cyperaceae and grass species supports the development of a peat bog, currently covering a large part of the lake (Teixeira et al., 2021). Simultaneously, charcoal counts exhibit that fires started to occur, probably not in Montagne d'Ambre, but more likely occurring in the low elevation areas surrounding the mountains. Such a change has also been corroborated by a second lake in Montagne d'Ambre, surrounded by rainforest (L. Mahasarika). Furthermore, at that time, both lakes also evidenced shallower conditions, showing that the increase in fires and human activity evidenced in the region also occurred under drier conditions (Montade et al. 2024).

2.3. Dating and age model

A first age-model depth model was initially built on the 11-m sediment core using 19 radiocarbon ages by Teixeira et al. (2021). A total of 8 new radiocarbon dates were added to the first 7 m to strengthen the Holocene section. Radiocarbon ages were calibrated using the SHcal20 calibration curve (Hogg et al., 2020). Then, to generate an age/depth model, a linear model was used and computed thanks to the package bacon in the RStudio (Blaauw, 2010).

2.4. Extraction of organic molecules

For Polycyclic Aromatic Hydrocarbons (PAHs) analysis, 49 samples were taken, freeze-dried, homogenised and sieved at 200 µm. A solid-liquid extraction was then performed on ca. 1 g of sediments as well as four cycles of extraction for 10 min by ultrasound with different solutions: 10 ml of a mixture of acetone/dichloromethane (DCM), 1-1 (v/v) for the first two cycles, and 10 ml of methanol for the last two. The extract was filtered (Teflon filters 20 µm) and evaporated under a nitrogen flow until around 1 ml. Molecules were separated into 3 fractions by SiO₂ column chromatography. Separation was performed using 8 ml hexane (apolar fraction including *n*-alkanes) for fraction 1; 5 ml heptane-DCM (98 :2, v/v), then 2 ml heptane-DCM for fraction 2; and 10 ml DCM-Methanol (1:1, v/v) for fraction 3. If pigment remained in fraction 1, a second separation by SiO₂ column chromatography was performed.

The fractions 1 and 2 were evaporated under a nitrogen flux and dymethylsulfoxide was used as a keeper and to change the solvent to methanol for the analysis.

2.5. PAH analyses and quality of the analyses

The analyses of fractions 1 and 2 were realised using High Performance Liquid Chromatography (Perkin Elmer HPLC device, serie 200) coupled to a fluorimeter detector (PE serie 200a). The separation was performed using a pre-column (EC 250/4.6 nucleosil 100-5 C18 PAHs) and a Macherey Nagel C18 column (EC 4/3 nucleosil 100-5 C18 PAHs) placed in an oven set at 30 °C. The analytic method described by Garagnon et al. (2024) was used. For quantification, 6 solutions of PAHs (2.4ng/ml to 100 ng/ml) have been analysed to compute the calibration line.

A total of 15 PAHs were analyzed: naphthalene (N), acenaphthene (Ace), fluorene (Flu), phenanthrene (Phe), anthracene (Ant), fluoranthene (Fla), pyrene (Pyr), benzo[a]anthracene (BaA), chrysene (Chr), benzo[e]pyrene (BeP), benzo[b]fluoranthene (BbF), benzo[k]fluoranthene (BkF), benzo[a]pyrene (BaP), benzo[ghi]perylene (BghiP), dibenzo[a,h]anthracene (DbahA), and indeno[1,2,3-cd]pyrene (IP). As Perylene (Per) coeluted with BbF and a large amount is contained in those sediments, BbF evolution will not be discussed in this study.



190 PAH physico-chemical characteristics allow them to be transported over long distances (Cabrerizo et al., 2014;
Halsall et al., 2001). However, lighter and smaller molecules will be transported further than heavier ones. In
addition, observations have shown that wet deposits are more significant than dry deposits (Marçais, 2017) and
that rainfall helps the scavenging of PAHs in lacustrine sediment (Denis et al., 2012). The lighter molecules, which
are more present in the gaseous phase, have a solubility coefficient greater than that of the heavier PAHs, which
are in the particulate phase. Therefore, we hypothesize that the long-distance PAHs record in the lacustrine core
195 would be dominated by lighter compounds scavenged from the atmosphere by rainfall. Thus, for this study, two
groups of PAHs will be distinguished according to their coefficient of solubility at 25°C (Garagnon et al., 2023).
The weakly hydrophobic group contains more hydrophilic PAHs with a solubility coefficient $> 10^{-2}$ mg.L⁻¹ (N,
Ace, Flu, Phe, Ant, Fla and Pyr). The highly hydrophobic group contains PAHs more hydrophobic with a solubility
coefficient $< 10^{-2}$ mg.L⁻¹ (BaA, Chr, BaP, BghiP, DbahA, IP).

200

The limit of quantification (LOQ) and limit of detection (LOD) were computed thanks to the slope coefficients (a)
and the y-intercept (b) of 10 calibration lines. A LOD and a LOQ were calculated for each PAH measured.

205 If the value of a PAH concentration in a sample is below the LOD, then the concentration is considered as null.
However, if the value of a PAH concentration in a sample is comprised between the value of the LOD and the the
LOQ, then its concentration is estimated equal to (Croghan and Egeghy, 2003).

210 During chemical procedures, blank controls were performed and potential contamination quantities were removed
from the sample results.

210

Moreover, two sets of 5 certified soils were extracted, and the efficiencies found have been applied to the measured
concentration to compensate for the loss by evaporation. The efficiencies can be found in the supplementary
material (Table SM 1).

215

3. Results

3.1. Age model

220 The calibrated ages are provided in Table 1 and the age model in Figure 2. The new age-depth model, built with 8
new radiocarbon dates, better constrained the Holocene, notably between 7000 and 5000 cal a BP. As for Teixeira
et al. (2021), several inverted dates were removed from the age-depth modelling during the last glacial termination
and the late glacial. The age-depth model is similar to the previous one, and the inverted ages are explained as the
result of old carbon input in the sediment, resulting from significant erosion during that period. Focusing on the
225 Holocene period, this new age-depth model provides a very robust chronology for this time period.

230



235

Table 1 : Date ¹⁴C used for the age-depth model of Lake Maudit realised with the package clam (Blaauw, 2010). Bold and italic lines are inversed age which are no taking account in the model.

lab ID	Age ¹⁴ C	error	depth (cm)
Sac A 61839/LM1B 213-214	-155	19	213.5
Poz-101233/LM1B-235	505	30	234.35
SacA61840/LM1B-255.5	1125	30	254.35
SacA61841/LM1B-286.5	1680	30	287.46
Poz-101234/LM1B-320	2225	30	321.46
Poz-97327/LM1B-382	2685	30	348.48
SacA61842/LM1B-418.5	3325	30	384.48
Poz-101235/LM1B-460	3775	35	426.28
SacA61843/LM1B-502.5	4340	30	467.03
SacA61844/LM1B-532.5	5210	30	497.55
Poz-97328/LM1B-549.5	5230	40	515.05
SacA61845/LM1B-593.5	6370	30	557.55
Poz-101236/LM1B-630	7800	40	596.93
SacA61846/LM1B-649.5	8555	40	615.93
Poz-106018/LM1B-670	8830	50	636.93
<i>Poz-101237/LM1B-708</i>	<i>10230</i>	<i>50</i>	<i>672.7</i>
<i>Poz-94285/LM1A-719</i>	<i>10300</i>	<i>60</i>	<i>686.26</i>
Poz-97329/LM1B-784.5	10280	60	750.99
<i>Poz-111303/LM1B-820</i>	<i>12120</i>	<i>60</i>	<i>786.49</i>
<i>Poz-97330/LM1B-857</i>	<i>12260</i>	<i>60</i>	<i>821.76</i>
<i>Poz-111270/LM1B-902</i>	<i>12900</i>	<i>60</i>	<i>869.1</i>
Poz-106099/LM1B-940	12180	60	905.24
Poz-97331/LM1B-1013	12930	60	972.93
<i>Poz-111271/LM1A-1033</i>	<i>31700</i>	<i>700</i>	<i>998.39</i>
<i>Poz-106100/LM1B-1035</i>	<i>23310</i>	<i>300</i>	<i>998.98</i>
<i>Poz-106101/LM1B-1055</i>	<i>20430</i>	<i>250</i>	<i>1018.98</i>
Poz-101239/LM1B-1070	19820	120	1033.98

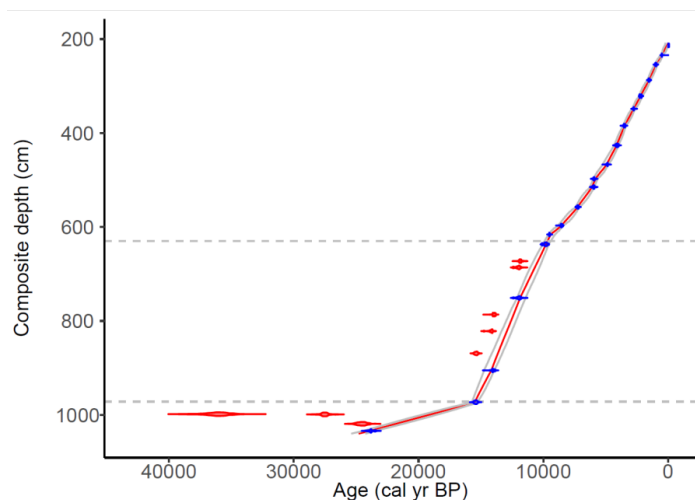


Figure 2 : Linear age-depth model of lake Maudit realised with the package clam (Blaauw, 2010). Red points are inversed age which are not taking into account in the model.

240

3.2. Quantity and evolution of PAH

245

PAH concentrations range from 5 to 582 $\text{ng.g}^{-1}_{\text{dw}}$ (Fig. 3) and exhibit three periods of significantly higher values: around 9500 cal a BP, 7400-5000 cal a BP, and over the last 500 years.

Over the Holocene, the hydrophilic PAHs (i.e., those with a $\log_{10}(\text{Solubility}) > -2$) are globally more abundant than hydrophobic PAHs (Fig. 3). However, the relative abundance of hydrophobic PAHs has begun to increase since 2800 cal a BP.

250

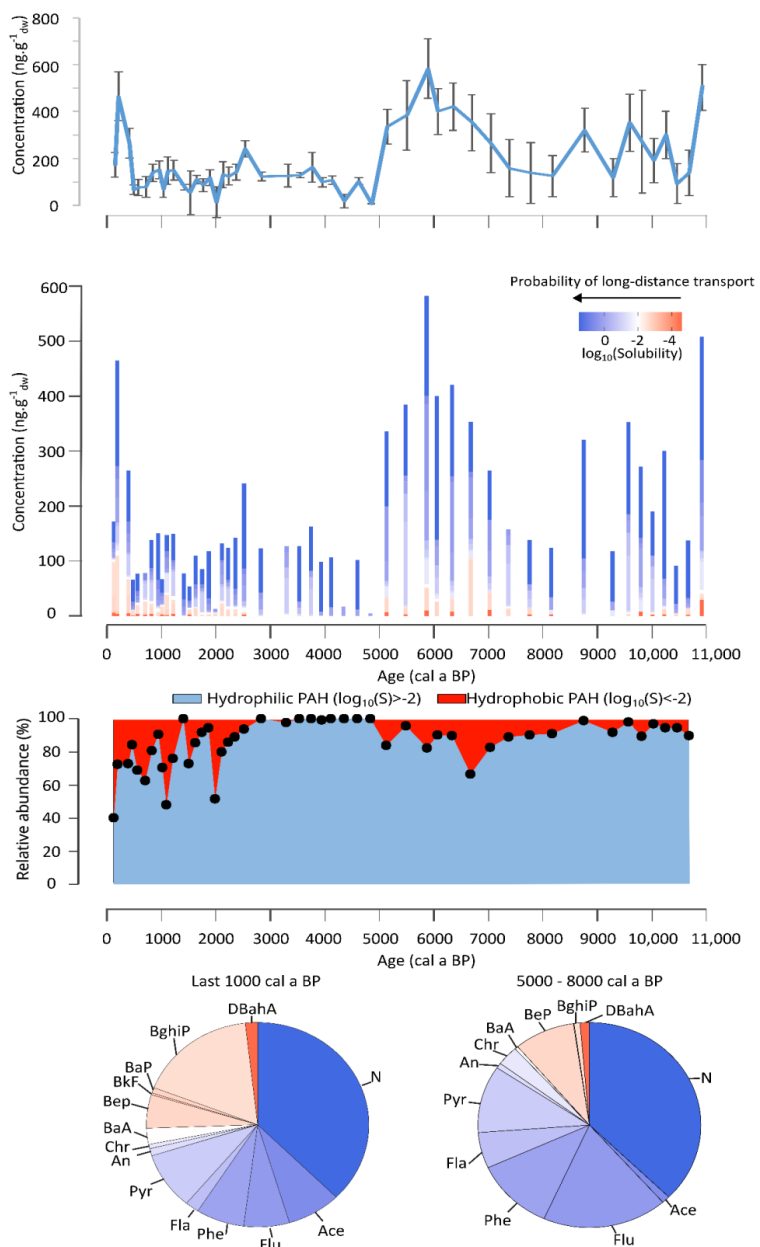
Hydrophilic PAHs are mainly composed of N, Flu, Phe, Fla, and Pyr (Fig. 3). Their highest concentrations are reported between 10,200 and 4800 cal a BP, reaching 479 $\text{ng.g}^{-1}_{\text{dw}}$ at 5800 cal a BP. Then, from 4800 to 4000 cal a BP, the hydrophilic concentration is low at around 100 $\text{ng.g}^{-1}_{\text{dw}}$. They reached 123 $\text{ng.g}^{-1}_{\text{dw}}$ at 3300 cal a BP before decreasing to 70 $\text{ng.g}^{-1}_{\text{dw}}$, with several wiggles. Finally, since 500 cal a BP, the concentrations show a marked rise.

255

Regarding the evolution of hydrophobic PAHs, similar trends can be observed, but with lower concentrations (Fig.3). However, no hydrophobic PAHs were found between 4800 and 2800 cal a BP. Since 2800 cal a BP, this group denotes an important increase in concentration since 2800 cal a BP, and reaches 127 $\text{ng.g}^{-1}_{\text{dw}}$ at 190 cal a BP. The PAH chemical features evolved over the Holocene. Indeed, between 5000 and 8000 cal a BP, hydrophobic PAHs are mainly composed of Chr, BeP, and BaA (Fig.2B), whereas since 2800 cal a BP, much heavier compounds (BghiP and DbahA) dominate (Fig. 2C).

260

265



270

Figure 3 : Variation of PAH concentration ($\text{ng}\cdot\text{g}^{-1}_{\text{dw}}$) in function of the solubility of PAH in lake Maudit, over the Holocene in concentration and in relative abundance. Mean of PAH relative abundance since 1000 cal a BP. Mean of PAH relative abundance between 8000 and 5000 cal a BP.

275

4. Discussion



4.1. PAH sources

280

4.1.1. Influence of biogenic PAHs

The PAH signal is commonly used to infer the type of fuel involved during a wildfire combustion (Ana Lúcia C. Lima et al., 2005). However, a growing set of evidence from regions suggests that certain PAHs, such as N and Phe, typically generated by wildfires in temperate areas, may also originate directly from the metabolic processes of living organisms (Grice et al., 2009; Krauss et al., 2005; Wakeham and Canuel, 2016; Wilcke et al., 2003, 2002, 2000). Perylen (Per) is an additional PAH that does not result from combustion but is exclusively generated by biological processes (Grice et al., 2009; Krauss et al., 2005; Marynowski et al., 2015; Wilcke et al., 2002) and is abundantly represented in our record. Perylene is a PAH comprising 5 rings, generated under anaerobic conditions (Grice et al., 2009; Wilcke et al., 2002). Although its production mechanisms remain debated (Li et al., 2022), its biological origin is broadly acknowledged and evidenced through the $\delta^{13}\text{C}$ values of the molecule (Bertrand et al., 2013; Grice et al., 2009; Li et al., 2022; Wilcke et al., 2002). Moreover, in tropical environments (Grice et al., 2009; Wilcke et al., 2002), perylene may also originate from termite nests (Krauss et al., 2005).

285

290

In Lake Maudit, the abundance of perylene increases with depth before 5000 cal a BP (Fig. SM 2). The depth dependence in lacustrine records suggests that diagenetic processes are also involved as production mechanisms. Furthermore, in Lake Maudit, perylene could account for up to 95% of the PAH abundance, which aligns with the elevated levels reported in other studies (Krauss et al., 2005).

295

To infer the origins of N and Phe in Lake Maudit, we analysed their signal patterns in comparison to signals of exclusively biological origin (Perylene) and those of purely combustion-derived origin (Pyr, Flu, Fla, Fig. SM 3). The patterns of N and Phe signals resemble those originating from pure fire combustion. However, N abundance seems to increase with depth. Therefore, we assume that Phe has a combustion origin, while a partially biological origin of N cannot be excluded.

300

4.1.2. Influence of local fire

We confronted our PAH data with the charcoal record (Teixeira et al. 2021; Fig. 4A, B and C). Both signal show distinct patterns between 12,000 and 2500 cal a BP. No charcoal was found, whereas the PAH concentration was at its highest values. From 2500 to 1000 cal a BP, few particles were observed. PAH concentration presented a small increase from 2500 cal a BP. Then from 1000 cal a BP, both signals have remained coherent over the past 1000 years, despite certain differences in detail. PAH and charcoal maximum concentrations occur at 740 cal a BP and 190 cal a BP, respectively. These results effectively demonstrate that charcoal particles $>160\ \mu\text{m}$ capture a proximal/local fire signal originating from a few km away, i.e., the drier, low-elevation dry forest/savanna zones where fires presently occur. These drier areas encircle the Montagne d'Ambre rainforest, within which fire currently remains absent in the core of the rainforest. This contrasts with PAHs, which can be transported over extended distances (several thousand kilometres), thereby representing a more regional signal (Cabrerizo et al., 2014; Halsall et al., 2001; Karp et al., 2020b; Miller et al., 2017; Vachula et al., 2022).

305

310

315

Other records of charcoal have been published for the late Holocene (Matsumoto and Burney, 1994; Montade et al., 2024; Reinhardt et al., 2022), including a second lake in Montagne d'Ambre (Lake Mahasarika), Nosy Be Island (Lake Amparahibe) and from northwest Madagascar (Lake Mitsinjo). All these records evidenced a general increase in fire occurrences starting a bit before the last millennium. Beyond the past two millennia, charcoal particles occur very rarely and are mostly absent from the sediment, showing very low fire frequency. Therefore, the northern region of Madagascar cannot be considered as a source of PAHs, particularly during the early and mid-Holocene, where Lake Maudit shows the highest values, but this would reflect more remote sources supplying

320



PAHs. Furthermore, in Lake Maudit, the concentration of the more hydrophobic PAHs was higher during the last millennium in comparison with the rest of the record. This means that the local source allows input of more hydrophobic PAH. This observation is consistent with those reported in remote places, where lighter PAHs were found compared to heavy PAHs (Cabrerizo et al., 2014; Halsall et al., 2001; Karp et al., 2020; Lima et al., 2005). PAHs likely originate from regional biomass burning and were transported atmospherically before deposition.

4.1.3. Where came from PAH during the Early and Mid-Holocene?

Three areas can be proposed to be the possible origins for PAHs beyond the vicinity of Lake Maudit: the southern region of Madagascar, Equatorial Asia/Australia, and East Africa. Over long distances, PAH are transported by wind. Therefore, an area can be a source of a PAH signal, depending on the wind regime that took place in the North of Madagascar.

Firstly, in the Lake Maudit PAH signals, a comparable global pattern between hydrophobic and hydrophilic PAHs is observed (Fig. 4A, C). We suppose that hydrophilic and hydrophobic PAHs have the same origin as there are similarities in their concentration variation. Between 8000 and 5000 cal a BP, the hydrophobic PAHs were predominantly composed of one of the lighter PAHs of this group (BeP), while particulate-phase PAHs (BaP, BghiP, DbahA) were nearly absent (Fig. 3C). The particulate phase PAHs are typically deposited in the proximity to the fire sources. In remote locations, only the lighter PAHs are detected (Cabrerizo et al., 2014; Halsall et al., 2001; Karp et al., 2020; Lima et al., 2005). Therefore, this implies that although distant, the fire source is not excessively far. Consequently, the Equatorial Asia/Australia source can be dismissed as a primary source.

Secondly, in the central part of Madagascar (Lake Tritrikevaly and Lake Kavitaha, cf ref. in Burney (1987), Fig. 1A) and in the southern region of Madagascar (in the Sainte-Luce area (Virah-Sawmy et al., 2010)), Fig. 1A), charcoal records allowed for documenting fire activity during the Holocene. In the central part, fires occurred frequently from the early to the mid-Holocene and during the past millennium (Fig. 4D). In the southeastern region (Sainte-Luce), fires only occurred during the Late Holocene. Therefore, fires occurred during the Holocene, which allowed PAH production. However, the wind regime separates the northern region from the central/southern regions of Madagascar (Chevalier et al., 2017; Gasse, 2000; Joly, 1941; Jury et al., 1995; Macron et al., 2016; Scroxton et al., 2023). Therefore, it is unlikely that PAHs in Lake Maudit originate from the central/southern regions of Madagascar.

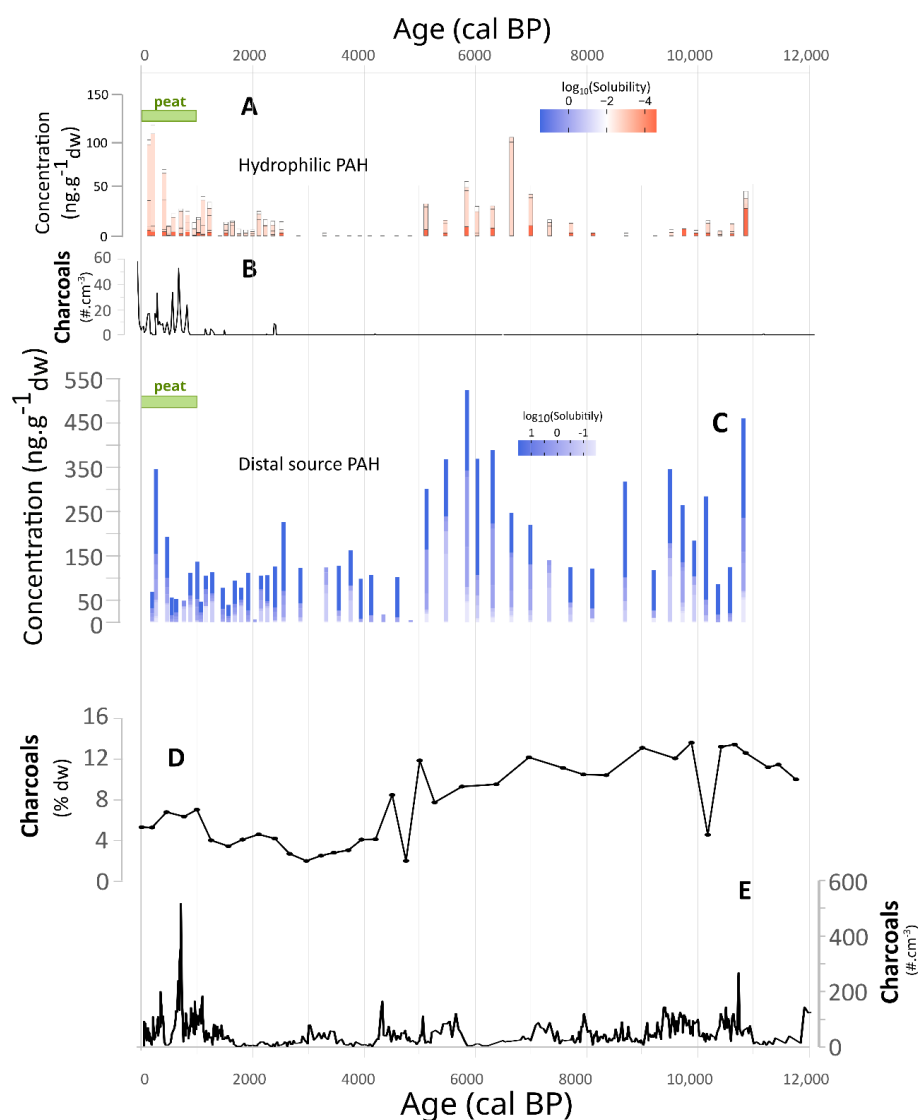
We therefore assume an East African origin for the long-distance transported PAHs observed in Lake Maudit cores. This hypothesis is further supported by i) the prevalence of wildfires in East Africa throughout the Holocene (Bremond et al., 2024; Karp et al., 2021) (Fig. 4E) and ii) the distinctive wind pattern that enables atmospheric masses to access northern Madagascar by crossing the East African landmass and the Mozambique Channel (Fig. 1B).

4.2. Decoupling between PAHs and fires

In East Africa, fire activity was reported during the Holocene (Aleman et al., 2025; Bremond et al., 2024; Karp et al., 2023). Its variability could influence the amount of emitted PAHs (Battistel et al., 2017; Karp et al., 2020a; Ana Lúcia C. Lima et al., 2005). In East Africa, different patterns of fire regime appear (Aleman et al., 2025; Karp et al., 2023). Fire activities did not necessarily diminish during the East African Humid Period (Karp et al., 2023). The fire regime depends on fuel availability, moisture content and land uses (Aleman et al., 2025; Karp et al., 2023). Holocene fire regimes have been inferred from Lake Tanganyika and Lake Victoria thanks to charcoal and PAH fluxes, respectively (Ivory and Russell, 2016; Karp et al., 2023). In Tanzania, the Lake Mosoko have the highest resolved charcoal record over the entire Holocene (Aleman et al., 2025). In the different site, the fire activity was distinct over the Holocene. At Lake Tanganyika, fire activity was huge at the beginning of the EAHP



370 until 11,000 cal a BP (Ivory and Russell, 2016; Karp et al., 2023). Then it remained low over the rest of the
 Holocene, contrary to Lake Victoria, where the fire activities decreased during the EAHP (Karp et al., 2023). Lake
 Masoko, record high value of charcoal accumulation between 10,700 and 9400 cal a BP (Aleman et al., 2025)
 (Fig. 4E). Then, they conclude that fire activity reaches a minimum at 6400 cal a BP before increasing again at
 5800 cal a BP. The fire activity reconstructed from the East Africa exhibits a pattern markedly distinct from the
 375 Lake Maudit PAH record during the early-mid Holocene. However, it is more likely that the PAHs present in Lake
 Maudit originated from various sources from East Africa. PAHs likely originate from regional biomass burning,
 but the variation was not due to fire activity variation.



380 **Figure 4 :** Comparison of Lake Maudit PAH concentration with fire signal over the Holocene. A. Concentration
 ($\text{ng.g}^{-1}_{\text{dw}}$) of hydrophobic PAH ($S < 0.01 \text{ mg.L}^{-1}$) in lake Maudit. B. Counting of charcoal and abundance of *Poacée*
 pollen in lake Maudit (Teixeira et al., 2021). C. Concentration ($\text{ng.g}^{-1}_{\text{dw}}$) of hydrophile PAH ($S > 0.01 \text{ mg.L}^{-1}$) in



lake Maudit. D. Counting of charcoal in lake Tritrikavely (Burney, 1987). D. Counting of charcoal in lake Masoko (Aleman et al. 2025).

4.3. Evidence for a precipitation-controlled PAH deposition

385

The hydrophilic PAHs identified in Lake Maudit sediments indicate a distal origin, likely East Africa. The cumulative concentration of those remote PAH peaks between 11,000 and 5000 cal a BP, before declining sharply (Fig. 4E). This period coincides with the well-documented EAHP.

390

In the past two decades, PAHs have increasingly been used as a palaeo-fire proxy (Argiriadis et al., 2024; Battistel et al., 2017; Callegaro et al., 2018; Denis et al., 2017, 2012; Karp et al., 2020b; Miller et al., 2017; Vachula et al., 2022). Subsequent studies suggest correlating PAH signals with arid periods, predicated on the premise that a drier climate would promote the incidence of wildfires (Battistel et al., 2017; Zhang et al., 2025). Consequently, it is challenging to correlate PAHs with climate solely based on wildfire occurrences. Furthermore, recent studies on

395

PAH dispersion patterns indicate a direct correlation between PAH deposition and precipitation. Marçais (2017) monitored PAH depositions near Lake La Muzelle in the French Alps, demonstrating that wet deposits account for up to 98% of the total PAH fallout. Denis et al. (2012) reached similar conclusions after comparing sedimentary PAHs with historical data, determining that rainfall tends to scavenge PAHs from the atmosphere. This mechanism has also been observed with black carbon, which is affected by the quantity of precipitation (Battistel et al., 2018).

400

The authors of those observations proposed that, regardless of atmospheric aerosol levels, PAH deposition is enhanced by water condensation, which tends to scavenge PAHs from the atmosphere. This process is particularly efficient for the most soluble PAH congeners, specifically those with peak concentrations in sediment during the African Humid Period. This leads us to hypothesise that the pre-anthropogenic deposition of aerosol-born PAHs from Africa to Lake Maudit might also be partly controlled by precipitation.

405

Indeed, past vegetation changes inferred from Lake Maudit evidence the influence of the EAHP in Northern Madagascar as recorded in East Africa. In particular, the emergence of the modern humid rainforest started from ca. 15 000 cal a BP and culminated in the early Holocene. This rainforest replaced montane forest, less water-demanding vegetation. The rainforest persisted through the Holocene until modern conditions. However, the increase in pioneer species indicated more disturbance from 5500 cal a BP, contemporaneously with an increase in shallow lake conditions, evidenced by the increase of aquatic pollen taxa, supporting a decrease in precipitation. While they cautiously also interpreted the increase in hardly-weathered major elements in the sediment as a consequence of elevated weathering rates of soils under more humid conditions during the EAHP (Fig. 5C) (Teixeira et al., 2021). Together, from 5500 cal a BP, results from Lake Maudit highlight the end of the EAHP

410

when a decrease in hydrophilic PAH is also observed in Lake Maudit. The tendency of a decrease in the water level was reinforced since 1000 cal a BP, as reflected by the development of a peat bog and the spread of Cyperaceae and Poaceae on the lake bank (Fig 5.5B). However, the increase in anthropogenic fires in the region during the past millennium, which influences the PAH input, prevents interpreting the PAH signal as a precipitation signal during this period (Fig. 5E). Then, over the last millennium, the PAH signal may also have been significantly influenced by local fire activity.

415

420

In addition, multiple Holocene records of precipitation have recently been published, derived from $\delta^{18}\text{O}$ of speleothems collected in northwestern Madagascar (Dawson et al., 2024; Voarintsoa et al., 2017; Wang et al., 2019) (Fig. 5D). Those studies also indicate wet conditions during the EAHP, which ended abruptly at 5500 cal. BP, and coincided with the decline in hydrophilic PAHs observed in Lake Maudit. The analysis of the speleothem

425



ANJ94-5 indicates that the transition towards drier conditions occurred later, approximately 4900 cal a BP. In this context, our data hence may indicate a significant decline in precipitation post 5500 cal a BP.

These observations tend to corroborate our hypothesis that the hydrophilic PAH signal reflects a precipitation signal.

430

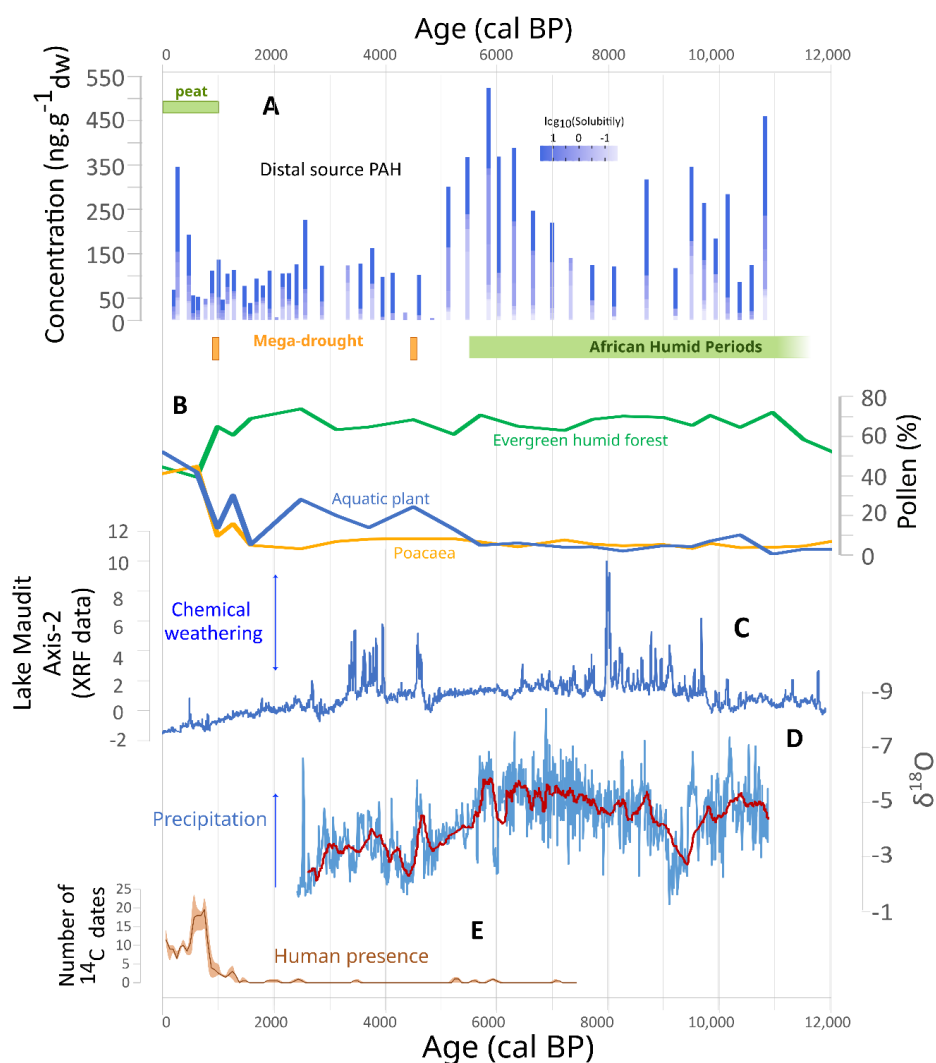


Figure 5: Comparison of Lake Maudit PAH concentration with precipitation signal over the Holocene. A. Concentration ($\text{ng.g}^{-1}_{\text{dw}}$) of hydrophilic PAH ($S < 0.01 \text{ mg.L}^{-1}$) in lake Maudit. B. Percentage of pollen counting in Lake Maudit (Teixeira et al., 2021). C. PCA axis-2 from XRF data in lake Maudit, inferred in terms of chemical weathering. (Teixeira et al., 2021) D. $\delta^{18}\text{O}$ variation in the speckthene AB-11 from Anjohibe cave, inferred in term of precipitation (Dawson et al., 2024). E. Number of ^{14}C dates inferred in terms of human presence (Douglass et al., 2019). Orange and green rectangle represents the span time of observed mega-drought (Li et al., 2018; Montade et al., 2023) and African Humid Period (Gasse, 2000; Tierney et al., 2011).

435

440



5. Conclusion

In this study, the concentrations in Polycyclic Aromatic Hydrocarbons (PAHs), which are molecules produced by incomplete combustion, have been measured. Those molecules, which could be stored in sedimentary archive, are usually used to infer palaeofires. In the North of Madagascar, fire activity was reduced over the last 1000 cal a BP. However, the concentrations in PAH present high values and significant variations over the Holocene, which means they represent a remote signal of fire activities. Those molecules come from East Africa, thanks to westerly winds that are set in motion when the ITCZ is its southern seasonal position. However, the signal of PAH differs from the fire activity signal but is similar to the one of precipitation. Precipitation in the North of Madagascar allows to scavenging of the atmosphere and trapping PAHs in lakes before being archived in sediments. These results challenge the direct interpretation of PAHs in terms of fire events and dry periods.

6. Acknowledgements

Some of the radiocarbon ages were obtained through the Artemis French AMS 14C dating program.

7. Author contribution

Conceptualization: EB, VM, CP, AF, GM ; Data curation: HB, VM ; Investigation: EB, APT, IB ; Supervision: AF, CP, GM ; Visualisation: EB, ATP ; Writing: EB, VM, CP, GM, APT, IB, HB, CGC, LB, FA.

8. Competing interests

The authors declare that they have no conflict of interest.

9. References

- Aleman, J.C., Garcin, Y., Vannière, B., Vullien, A., Williamson, D., Carcaillet, C., 2025. Evenness peaks in fire-resilient vegetation preceded ecosystem shifts in East Africa. *Environ. Res. Lett.* 20, 074010. <https://doi.org/10.1088/1748-9326/add8a4>
- Argiriadis, E., Denniston, R.F., Ondei, S., Bowman, D.M.J.S., Genuzio, G., Nguyen, H.Q.A., Thompson, J., Baltieri, M., Azenon, J., Cugley, J., Woods, D., Humphreys, W.F., Barbante, C., 2024. Polycyclic aromatic hydrocarbons in tropical Australian stalagmites: a framework for reconstructing paleofire activity. *Geochimica et Cosmochimica Acta* 366, 250–266. <https://doi.org/10.1016/j.gca.2023.11.033>
- Battistel, D., Argiriadis, E., Kehrwald, N., Spigariol, M., Russell, J.M., Barbante, C., 2017. Fire and human record at Lake Victoria, East Africa, during the Early Iron Age: Did humans or climate cause massive ecosystem changes? *The Holocene* 27, 997–1007. <https://doi.org/10.1177/0959683616678466>
- Battistel, D., Kehrwald, N.M., Zennaro, P., Pellegrino, G., Barbaro, E., Zangrando, R., Pedeli, X.X., Varin, C., Spolaor, A., Vallelonga, P.T., Gambaro, A., Barbante, C., 2018. High-latitude Southern Hemisphere fire history during the mid- to late Holocene (6000–750 BP). *Climate of the Past* 14, 871–886. <https://doi.org/10.5194/cp-14-871-2018>
- Bertrand, O., Montargès-Pelletier, E., Mansuy-Huault, L., Losson, B., Faure, P., Michels, R., Pernot, A., Arnaud, F., 2013. A possible terrigenous origin for perylene based on a sedimentary record of a pond (Lorraine, France). *Organic Geochemistry* 58, 69–77. <https://doi.org/10.1016/j.orggeochem.2013.02.015>
- Blaauw, M., 2010. Methods and code for ‘classical’ age-modelling of radiocarbon sequences. *Quaternary Geochronology* 5, 512–518. <https://doi.org/10.1016/j.quageo.2010.01.002>
- Bremond, L., Aleman, J.C., Favier, C., Blarquez, O., Colombaroli, D., Connor, S.E., Cordova, C.E., Courtney-Mustaphi, C., Dabengwa, A.N., Gil-Romera, G., Gosling, W.D., Hamilton, T., Montade, V., Razafimanantsoa, A.H.I., Power, M.J., Razanatsoa, E., Yabi, I., Vannière, B., 2024. Past fire dynamics in sub-Saharan Africa



- during the last 25,000 years: Climate change and increasing human impacts. *Quaternary International* 711, 49–58. <https://doi.org/10.1016/j.quaint.2024.07.012>
- 490 Burney, D.A., 1987. Late Quaternary stratigraphic charcoal records from Madagascar. *Quaternary Research* 28, 274–280. [https://doi.org/10.1016/0033-5894\(87\)90065-2](https://doi.org/10.1016/0033-5894(87)90065-2)
- Cabrerizo, A., Galbán-Malagón, C., Del Vento, S., Dachs, J., 2014. Sources and fate of polycyclic aromatic hydrocarbons in the Antarctic and Southern Ocean atmosphere. *Global Biogeochemical Cycles* 28, 1424–1436. <https://doi.org/10.1002/2014GB004910>
- 495 Callegaro, A., Battistel, D., Kehrwald, N.M., Matsubara Pereira, F., Kirchgeorg, T., Villoslada Hidalgo, M. del C., Bird, B.W., Barbante, C., 2018. Fire, vegetation, and Holocene climate in a southeastern Tibetan lake: a multi-biomarker reconstruction from Paru Co. *Climate of the Past* 14, 1543–1563. <https://doi.org/10.5194/cp-14-1543-2018>
- Chevalier, M., Brewer, S., Chase, B.M., 2017. Qualitative assessment of PMIP3 rainfall simulations across the eastern African monsoon domains during the mid-Holocene and the Last Glacial Maximum. *Quaternary Science Reviews* 156, 107–120. <https://doi.org/10.1016/j.quascirev.2016.11.028>
- 500 Croghan, W., Egeghy, P., 2003. *Methods of Dealing with Values Below the Limit of Detection using SAS Carry*.
- Daniau, A.-L., Brücher, T., 2016. Fire, climate and biomes—towards a better understanding of this complex relationship. *Past Global Change Magazine* 24, 79–79.
- 505 Dawson, R.R., Burns, S.J., Tiger, B.H., McGee, D., Faina, P., Scroxton, N., Godfrey, L.R., Ranivoharimanana, L., 2024. Zonal control on Holocene precipitation in northwestern Madagascar based on a stalagmite from Anjohibe. *Sci Rep* 14, 5496. <https://doi.org/10.1038/s41598-024-55909-6>
- Denis, E.H., Pedentchouk, N., Schouten, S., Pagani, M., Freeman, K.H., 2017. Fire and ecosystem change in the Arctic across the Paleocene–Eocene Thermal Maximum. *Earth and Planetary Science Letters* 467, 149–156. <https://doi.org/10.1016/j.epsl.2017.03.021>
- 510 Denis, E.H., Toney, J.L., Tarozo, R., Scott Anderson, R., Roach, L.D., Huang, Y., 2012. Polycyclic aromatic hydrocarbons (PAHs) in lake sediments record historic fire events: Validation using HPLC-fluorescence detection. *Organic Geochemistry* 45, 7–17. <https://doi.org/10.1016/j.orggeochem.2012.01.005>
- 515 Doskey, P.V., Talbot, R.W., 2000. Sediment chronologies of atmospheric deposition in a precipitation-dominated seepage lake. *Limnology and Oceanography* 45, 895–904. <https://doi.org/10.4319/lo.2000.45.4.0895>
- Douglass, K., Hixon, S., Wright, H.T., Godfrey, L.R., Crowley, B.E., Manjakahery, B., Rasolondrainy, T., Crossland, Z., Radimilahy, C., 2019. A critical review of radiocarbon dates clarifies the human settlement of Madagascar. *Quaternary Science Reviews* 221, 105878. <https://doi.org/10.1016/j.quascirev.2019.105878>
- 520 Garagnon, J., Naffrechoux, E., Perrette, Y., Dumont, E., Branchu, P., Querleux, J., Monvoisin, G., Pin, M., Tisserand, D., Pons-Branchu, E., 2024. Impact of land-use on PAH transfer in sub-surface water as recorded by CaCO₃ concretions in urban underground structures (Paris, France). *Environmental Pollution* 357, 124437. <https://doi.org/10.1016/j.envpol.2024.124437>
- 525 Garagnon, J., Perrette, Y., Naffrechoux, E., Pons-Branchu, E., 2023. Polycyclic aromatic hydrocarbon record in an urban secondary carbonate deposit over the last three centuries (Paris, France). *Science of The Total Environment* 905, 167429. <https://doi.org/10.1016/j.scitotenv.2023.167429>
- Gasse, F., 2000. Hydrological changes in the African tropics since the Last Glacial Maximum. *Quaternary Science Reviews* 19, 189–211. [https://doi.org/10.1016/S0277-3791\(99\)00061-X](https://doi.org/10.1016/S0277-3791(99)00061-X)
- 530 Godfrey, L.R., Scroxton, N., Crowley, B.E., Burns, S.J., Sutherland, M.R., Pérez, V.R., Faina, P., McGee, D., Ranivoharimanana, L., 2019. A new interpretation of Madagascar’s megafaunal decline: The “Subsistence Shift Hypothesis.” *Journal of Human Evolution* 130, 126–140. <https://doi.org/10.1016/j.jhevol.2019.03.002>



- Grice, K., Lu, H., Atahan, P., Asif, M., Hallmann, C., Greenwood, P., Maslen, E., Tulipani, S., Williford, K., Dodson, J., 2009. New insights into the origin of perylene in geological samples. *Geochimica et Cosmochimica Acta* 73, 6531–6543. <https://doi.org/10.1016/j.gca.2009.07.029>
- 535 Halsall, C.J., Sweetman, A.J., Barrie, L.A., Jones, K.C., 2001. Modelling the behaviour of PAHs during atmospheric transport from the UK to the Arctic. *Atmospheric Environment* 35, 255–267. [https://doi.org/10.1016/S1352-2310\(00\)00195-3](https://doi.org/10.1016/S1352-2310(00)00195-3)
- Hogg, A.G., Heaton, T.J., Hua, Q., Palmer, J.G., Turney, C.S., Southon, J., Bayliss, A., Blackwell, P.G., Boswijk, G., Ramsey, C.B., Pearson, C., Petchey, F., Reimer, P., Reimer, R., Wacker, L., 2020. SHCal20 Southern Hemisphere Calibration, 0–55,000 Years cal BP. *Radiocarbon* 62, 759–778. <https://doi.org/10.1017/RDC.2020.59>
- 540 IPCC, 2022. *Climate Change 2022: Impacts, Adaptation and Vulnerability (Contribution of Working Group II to the Sixth Assessment Report of the Intergovernmental Panel on Climate Change)*, [H.-O. Pörtner, D.C. Roberts, M. Tignor, E.S. Poloczanska, K. Mintenbeck, A. Alegría, M. Craig, S. Langsdorf, S. Löschke, V. Möller, A. Okem, B. Rama (eds.)]. Cambridge University Press. Cambridge University Press, Cambridge, UK and New York, NY, USA, 3056 pp.
- Ivory, S.J., Russell, J., 2016. Climate, herbivory, and fire controls on tropical African forest for the last 60ka. *Quaternary Science Reviews* 148, 101–114. <https://doi.org/10.1016/j.quascirev.2016.07.015>
- Joly, F., 1941. Les climats de Madagascar. *L'Information Géographique* 5, 76–80. <https://doi.org/10.3406/ingeo.1941.5092>
- 550 Jury, M.R., Parker, B.A., Raholijao, N., Nassor, A., 1995. Variability of summer rainfall over Madagascar: Climatic determinants at interannual scales. *International Journal of Climatology* 15, 1323–1332. <https://doi.org/10.1002/joc.3370151203>
- Karp, A., Uno, K., Berke, M., Russell, J., Scholz, C., Faith, J., Staver, A.C., 2021. Savanna Fire Activity Responds Heterogeneously to Rainfall Shifts During the African Humid Period 2021, PP13A-10.
- 555 Karp, A.T., Holman, A.I., Hopper, P., Grice, K., Freeman, K.H., 2020a. Fire distinguishers: Refined interpretations of polycyclic aromatic hydrocarbons for paleo-applications. *Geochimica et Cosmochimica Acta* 289, 93–113. <https://doi.org/10.1016/j.gca.2020.08.024>
- Karp, A.T., Holman, A.I., Hopper, P., Grice, K., Freeman, K.H., 2020b. Fire distinguishers: Refined interpretations of polycyclic aromatic hydrocarbons for paleo-applications. *Geochimica et Cosmochimica Acta* 289, 93–113. <https://doi.org/10.1016/j.gca.2020.08.024>
- 560 Karp, A.T., Uno, K.T., Berke, M.A., Russell, J.M., Scholz, C.A., Marlon, J.R., Faith, J.T., Staver, A.C., 2023. Nonlinear rainfall effects on savanna fire activity across the African Humid Period. *Quaternary Science Reviews* 304, 107994. <https://doi.org/10.1016/j.quascirev.2023.107994>
- Krauss, M., Wilcke, W., Martius, C., Bandeira, A.G., Garcia, M.V.B., Amelung, W., 2005. Atmospheric versus biological sources of polycyclic aromatic hydrocarbons (PAHs) in a tropical rain forest environment. *Environmental Pollution* 135, 143–154. <https://doi.org/10.1016/j.envpol.2004.09.012>
- 565 Li, H., Sinha, A., Anquetil André, A., Spötl, C., Vonhof, H.B., Meunier, A., Kathayat, G., Duan, P., Voarintsoa, N.R.G., Ning, Y., Biswas, J., Hu, P., Li, X., Sha, L., Zhao, J., Edwards, R.L., Cheng, H., 2020. A multimillennial climatic context for the megafaunal extinctions in Madagascar and Mascarene Islands. *Science Advances* 6, eabb2459. <https://doi.org/10.1126/sciadv.abb2459>
- 570 Li, Z., Huang, H., Yan, G., Xu, Y., George, S.C., 2022. Occurrence and origin of perylene in Paleogene sediments from the Tasmanian Gateway, Australia. *Organic Geochemistry* 168, 104406. <https://doi.org/10.1016/j.orggeochem.2022.104406>
- Lima, Ana Lúcia C., Farrington, J.W., Reddy, C.M., 2005. Combustion-Derived Polycyclic Aromatic Hydrocarbons in the Environment—A Review. *Environmental Forensics* 6, 109–131. <https://doi.org/10.1080/15275920590952739>
- 575



- Lima, Ana Lúcia C., Farrington, J.W., Reddy, C.M., 2005. Combustion-Derived Polycyclic Aromatic Hydrocarbons in the Environment—A Review. *Environmental Forensics* 6, 109–131. <https://doi.org/10.1080/15275920590952739>
- 580 Macron, C., Richard, Y., Garot, T., Bessafi, M., Pohl, B., Ratiarison, A., Razafindrabe, A., 2016. Intraseasonal Rainfall Variability over Madagascar. *Monthly Weather Review* 144, 1877–1885. <https://doi.org/10.1175/MWR-D-15-0077.1>
- Marçais, J., 2017. Transferts des polluants organiques persistants de l’atmosphère aux milieux aquatiques de montagne (These de doctorat). Université Grenoble Alpes (ComUE).
- 585 Marynowski, L., Smolarek, J., Hautevelle, Y., 2015. Perylene degradation during gradual onset of organic matter maturation. *International Journal of Coal Geology*, 65th Annual Meeting of ICCP and 30th Annual Meeting of TSOP 139, 17–25. <https://doi.org/10.1016/j.coal.2014.04.013>
- Matsumoto, K., Burney, D.A., 1994. Late Holocene environments at Lake Mitsinjo, northwestern Madagascar. *The Holocene* 4, 16–24. <https://doi.org/10.1177/095968369400400103>
- 590 Miller, D.R., Castañeda, I.S., Bradley, R.S., MacDonald, D., 2017. Local and regional wildfire activity in central Maine (USA) during the past 900 years. *J Paleolimnol* 58, 455–466. <https://doi.org/10.1007/s10933-017-0002-z>
- Montade, V., Bremond, L., Teixeira, H., Kasper, T., Daut, G., Rouland, S., Rasoamanana, E., Ramavovolona, P., Favier, C., Arnaud, F., Radespiel, U., Behling, H., 2024. Montane rainforest dynamics under changes in climate and human impact during the past millennia in northern Madagascar. *R Soc Open Sci.* 11, 230930. <https://doi.org/10.1098/rsos.230930>
- 595 Reinhardt, A.L., Kasper, T., Lochner, M., Bliedtner, M., Krahn, K.J., Haberzettl, T., Shumilovskikh, L., Rahobisoa, J.-J., Zech, R., Favier, C., Behling, H., Bremond, L., Daut, G., Montade, V., 2022. Rain Forest Fragmentation and Environmental Dynamics on Nosy Be Island (NW Madagascar) at 1300 cal BP Is Attributable to Intensified Human Impact. *Frontiers in Ecology and Evolution* 9.
- 600 Scroton, N., Burns, S.J., McGee, D., Godfrey, L.R., Ranivoharimanana, L., Faina, P., Tiger, B.H., 2023. Hydroclimate variability in the Madagascar and Southeast African summer monsoons at the Mid- to Late-Holocene transition. *Quaternary Science Reviews* 300, 107874. <https://doi.org/10.1016/j.quascirev.2022.107874>
- Strobel, P., Henning, T., Bliedtner, M., Mosher, S.G., Rahimova, H., Haberzettl, T., Kirsten, K.L., Lehndorff, E., Power, M.J., Zech, M., Zech, R., 2024. Holocene fire dynamics and their climatic controls on the southern Cape coast of South Africa - A 7.2 ka multi-proxy record from the peatland Vankervelsvlei. *Quaternary Science Reviews* 325, 108464. <https://doi.org/10.1016/j.quascirev.2023.108464>
- 605 Teixeira, H., Montade, V., Salmons, J., Metzger, J., Bremond, L., Kasper, T., Daut, G., Rouland, S., Ranarilalaitiana, S., Rakotondravony, R., Chikhi, L., Behling, H., Radespiel, U., 2021. Past environmental changes affected lemur population dynamics prior to human impact in Madagascar. *Commun Biol* 4, 1–10. <https://doi.org/10.1038/s42003-021-02620-1>
- 610 Thevenon, F., 2003. Les résidus carbonés de feux dans les sédiments: Implications méthodologiques, climatiques et anthropiques.
- Tierney, J.E., Lewis, S.C., Cook, B.I., LeGrande, A.N., Schmidt, G.A., 2011. Model, proxy and isotopic perspectives on the East African Humid Period. *Earth and Planetary Science Letters* 307, 103–112. <https://doi.org/10.1016/j.epsl.2011.04.038>
- 615 Vachula, R.S., Karp, A.T., Denis, E.H., Balascio, N.L., Canuel, E.A., Huang, Y., 2022. Spatially calibrating polycyclic aromatic hydrocarbons (PAHs) as proxies of area burned by vegetation fires: Insights from comparisons of historical data and sedimentary PAH fluxes. *Palaeogeography, Palaeoclimatology, Palaeoecology* 596, 110995. <https://doi.org/10.1016/j.palaeo.2022.110995>
- 620 Vallet-Coulomb, C., Gasse, F., Robison, L., Ferry, L., Van Campo, E., Chalié, F., 2006. Hydrological modeling of tropical closed Lake Ihotry (SW Madagascar): Sensitivity analysis and implications for paleohydrological reconstructions over the past 4000 years. *Journal of Hydrology, Water Resources in Regional Development: The Okavango River* 331, 257–271. <https://doi.org/10.1016/j.jhydrol.2006.05.026>



- 625 Virah-Sawmy, M., Willis, K.J., Gillson, L., 2010. Evidence for drought and forest declines during the recent megafaunal extinctions in Madagascar. *Journal of Biogeography* 37, 506–519. <https://doi.org/10.1111/j.1365-2699.2009.02203.x>
- 630 Voarintsoa, N.R.G., Railsback, L.B., Brook, G.A., Wang, L., Kathayat, G., Cheng, H., Li, X., Edwards, R.L., Rakotondrazafy, A.F.M., Madison Razanatseheno, M.O., 2017. Three distinct Holocene intervals of stalagmite deposition and nondeposition revealed in NW Madagascar, and their paleoclimate implications. *Climate of the Past* 13, 1771–1790. <https://doi.org/10.5194/cp-13-1771-2017>
- Wakeham, S.G., Canuel, E.A., 2016. Biogenic polycyclic aromatic hydrocarbons in sediments of the San Joaquin River in California (USA), and current paradigms on their formation. *Environ Sci Pollut Res* 23, 10426–10442. <https://doi.org/10.1007/s11356-015-5402-x>
- 635 Wang, L., Brook, G.A., Burney, D.A., Voarintsoa, N.R.G., Liang, F., Cheng, H., Edwards, R.L., 2019. The African Humid Period, rapid climate change events, the timing of human colonization, and megafaunal extinctions in Madagascar during the Holocene: Evidence from a 2m Anjohibe Cave stalagmite. *Quaternary Science Reviews* 210, 136–153. <https://doi.org/10.1016/j.quascirev.2019.02.004>
- 640 Wilcke, W., Amelung, W., Krauss, M., Martius, C., Bandeira, A., Garcia, M., 2003. Polycyclic aromatic hydrocarbon (PAH) patterns in climatically different ecological zones of Brazil. *Organic Geochemistry* 34, 1405–1417. [https://doi.org/10.1016/S0146-6380\(03\)00137-2](https://doi.org/10.1016/S0146-6380(03)00137-2)
- Wilcke, W., Amelung, W., Martius, C., Garcia, M.V.B., Zech, W., 2000. Biological Sources of Polycyclic Aromatic Hydrocarbons (PAHs) in the Amazonian Rain Forest. *Journal of Plant Nutrition and Soil Science* 163, 27–30. [https://doi.org/10.1002/\(SICI\)1522-2624\(200002\)163:1%3C27::AID-JPLN27%3E3.0.CO;2-E](https://doi.org/10.1002/(SICI)1522-2624(200002)163:1%3C27::AID-JPLN27%3E3.0.CO;2-E)
- 645 Wilcke, W., Krauss, M., Amelung, W., 2002. Carbon Isotope Signature of Polycyclic Aromatic Hydrocarbons (PAHs): Evidence for Different Sources in Tropical and Temperate Environments? *Environ. Sci. Technol.* 36, 3530–3535. <https://doi.org/10.1021/es020032h>
- 650 Yamamoto, M., Wang, F., Irino, T., Yamada, K., Haraguchi, T., Nakamura, H., Gotanda, K., Yonenobu, H., Leipe, C., Chen, X.-Y., Tarasov, P.E., 2022. Environmental evolution and fire history of Rebun Island (Northern Japan) during the past 17,000 years based on biomarkers and pyrogenic compound records from Lake Kushu. *Quaternary International* 623, 8–18. <https://doi.org/10.1016/j.quaint.2021.09.015>
- Zhang, C., Qiu, Y., Wang, C., Fan, Q., Feng, Z., Zou, X., 2025. Pyrogenic carbon records of Holocene fire dynamics in the Yellow River Basin: Climate change and human activity forcing. *Palaeogeography, Palaeoclimatology, Palaeoecology* 659, 112626. <https://doi.org/10.1016/j.palaeo.2024.112626>